行政院國家科學委員會專題研究計畫　成果報告

傳輸線之面積、時間延遲、功率及雜訊最佳化(2/2)

計畫類別：個別型計畫
計畫編號：NSC92-2215-E-002-016-
執行期間：92 年 08 月 01 日至 93 年 07 月 31 日
執行單位：國立臺灣大學電子工程學研究所

計畫主持人：張耀文

報告類型：完整報告

處理方式：本計畫可公開查詢

中　華　民　國 93 年 12 月 20 日

傳輸線之面積、時間延遲、功率及雜訊最佳化

Area, Delay, Power, and Noise Optimization for Transmission Lines

計畫編號：NSC 92-2215-E-002-016

執行期限：92 年 8 月 1 日至 93 年 7 月 31 日

主持人：張耀文教授　國立臺灣大學電子工程學研究所

一、中文摘要

在深次微米設計中，當操作頻率到達數千赫茲時，晶片上面的電感效應已經不能再被忽略。因此，如何去精確地萃取出來傳輸連線結構的阻抗跟電感值變得十分重要。大部份以前的阻抗跟電感萃取著重在矩形切割的研究上，但是隨著時代的進步，有許多非一般性結構的晶片，例如 X-結構與 Y-結構連線結構已經被發表出來或是可以提供製造。很明顯一般的矩形切割方式對於這些特殊的連線結構已經不敷使用，所以在這個計畫中，我們提出了一個用三角形切割方式配合面積分方法來處理阻抗萃取問題，最後我們會跟這方面有名的軟體來做驗証，証明我們方法的正確性以及較多的彈性。

關鍵詞：電感，面積分，萃取，一般連線結構

二、英文摘要(Abstract)

As the operation frequency reaches gigahertz in very deepsubmicron designs, the effect of on-chip inductance on circuit performance can no longer be neglected. Therefore, it is desired to extract transmission-line impedance and inductance accurately. Most of the previous works on impedance and inductance extraction are based on rectangular discretization which has been shown effective for the classical Manhattan based IC interconnect structures. As technology advances, however, more general IC interconnect structures, such as the X-based and Ybased interconnect structures, have been introduced or even already in production. Those general interconnect structures allow wires to be routed with non-Manhattan shapes. For the non-Manhattan interconnect structures, rectangular discretization is obviously not sufficient. In this project, we propose to use the surface integral formulation with triangular discretization to extract impedance and inductance for the general IC transmission-line structures. Comparative studies with the famous FASTHENRY, FASTIMP, and IE3D show that our approach is flexible and effective.

Keywords: inductance, surface integral, extraction, general interconnect structures

三、背景和目的

1. Background

In high-performance circuit designs, on-chip inductance has become increasingly more significant due to faster rise times, lower resistance, and lower capacitance [2] [9]. Wider wires are frequently encountered in clock distribution networks and in higher metal layers [15]. Those wires are low resistance lines that can exhibit significant inductive effects. Furthermore, performance requirements are pushing the introduction of new materials such as copper interconnect for low resistance interconnect and new dielectrics to reduce interconnect capacitance [25]. These technological advances increase the importance of inductance. Therefore, it is desired to extract transmission interconnect inductance and impedance accurately for high-performance circuits.

There exist many famous works in the literature on accurate inductance and impedance extraction, such as FastImp [10] [26] and FastHenry [14] [21]. Most of the previous works are based on rectangular discretization—rectangular panel discretization using the surface integral formulation [7] [10] [26] or filament discretization using the volume integral formulation. For example, FastImp uses the surface integral formulation with rectangular panel discretization. FastImp divides conductors into many rectangular panels and computes the field on each panel. According to the field, the incident current can be computed, and thus the impedance can be extracted. In contrast, FastHenry uses the volume integral formulation with filament discretization. It cuts conductors into many filaments. Current of each filament is considered as a constant. After solving the volume integral formulae, the current and impedance of every filament can be computed.

Both of FastImp and FastHenry can effectively extract the impedance of a conductor with the Manhanttan (rectilinear) structure. However, with the rectangular discretization, they may not be effective enough for handling non-Manhattan interconnect structures. As technology advances, however, more general IC interconnect structures, such as the X-based [18] and Y-based [6] interconnect structures, have been introduced or even already in production. Those general interconnect structures allow wires to be routed with non-Manhattan shapes. For the non-Manhattan interconnect structures, classical rectangular discretization is obviously not sufficient.

2. Objective

In this project, we propose to use the surface integral formulation with triangular discretization to extract impedance and inductance for the general IC transmission-line structures for high-speed circuit designs. Since triangles are the most fundamental polygon, triangular discretization is more flexible and powerful in geometry discretization, e.g., for X-based or Y-based interconnect structures. Further, the surface integral formulation is generally considered more accurate than the volume integral formulation at the high-frequency domain.

四、研究方法

1. Preliminaries

We first introduce some preliminaries for our triangular discretization. Consider a homogeneous circuit system of multiple conductors with constant permittivity ε, permeability μ, and conductivity σ. Let E be an electric field. Using the surface integral formulation proposed in [7] [10] [26], for every conductor we have a vector Helmhotz equation for $\vec{E}$ as follows:

$$\nabla^2 \vec{E} - i\omega\mu\sigma\vec{E} = 0. \tag{1}$$

Applying Green's second vector identity [4],

$$\int_V (\vec{Q}\cdot\nabla\times\nabla\times\vec{P} - \vec{P}\cdot\nabla\times\nabla\times\vec{Q})dV = \oint_S (\vec{P}\times\nabla\times\vec{Q} - \vec{Q}\times\nabla\times\vec{P}), \tag{2}$$

into Equation (1), we have

$$\int_{S_i} G_1(x,y)\frac{\partial \vec{E}(y)}{\partial n_y}dy - \int_{S_i} \frac{\partial G_1(x,y)}{\partial n_y}\vec{E}(y)dy = \vec{E}(x) \tag{3}$$

where G(x, y) is Green's function which is given by

$$G_1(x,y) = \frac{e^{iK_1|x-y|}}{4\pi|x-y|}, K_1 = \sqrt{-i\omega\mu\sigma_k},$$

where $\vec{P}$ and $\vec{Q}$ are two vector functions that are continuous and have continuous first and second derivatives at all points of volume V and its surface S. Here, $\nabla\times$ denotes taking curl.

Applying Equation (2) into another vector Helmhotz equation

$$\nabla^2 \vec{E} = i\omega\mu J, \tag{4}$$

where J is the current density, we get

$$\int_S G_0(x,y)\frac{\partial \vec{E}(y)}{\partial n_y}dy - \int_S \frac{\partial G_1(x,y)}{\partial n_y}\vec{E}(y)dy + \nabla\psi(x) = 0, \tag{5}$$

and

$$G_0(x,y) = \frac{1}{4\pi|x-y|},$$

where Si is the surface of the i-th conductor, and S is the union of all surfaces. Here, φ denotes the potential on the vertices, n is the outward normal unit vector on the conductor surface, and ω is the angle frequency.

We have the following two formulae:

$$\nabla\cdot E = 0 \text{ (current conservation)} \tag{6}$$

and

$$\int_S G_0(x,y)\rho_s(y)dy = \varepsilon\psi(x), x, y \in S \text{ (scalar potential)}, \tag{7}$$

where ρ_S is the charge on the surface. Here we also have three boundary conditions, as illustrated in Figure 1:

- Panels in the non-contact surfaces: $E_n = \frac{i\omega\rho}{\sigma}$ (Electro-Magnetic-Quasi-Statics, EMQS) and $E_n = 0$ (Magneto-Quasi-Statics, MQS);
- Panels in the contact surfaces: apply $\frac{\partial E_n}{\partial n} = 0$; here, En is the electrical field in the normal direction;
- Panels in the contact surfaces: ψ is set to ψ_+ or ψ_-.

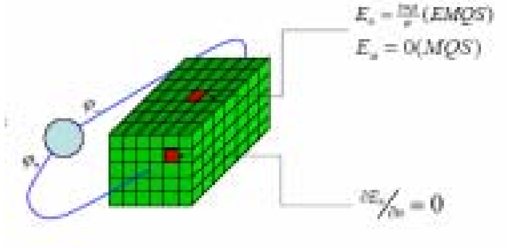

Figure 1: Contact and non-contact surface boundary conditions.

2. Discretization

In order to solve the whole system, we discretize the equation. We consider that there are many surfaces in a 3-D IC interconnect. For each surface, we can discretize it into many panels and vertices.

The major difference between our work and the previous works is the way of discretization. Traditional IC interconnects only contain vertical and horizontal wires (i.e., Manhattan/rectilinear interconnects). Therefore, previous works focus on the rectangular discretization into rectangular panels or filaments [7] [10] [26]. With the rectangular discretization, the previous works may not be effective enough for handling non-Manhattan interconnect structures, such as the X-based [18] and Y-based [6] interconnect structures. For the non-Manhattan interconnect structures, classical rectangular discretization is obviously not sufficient. In order to effectively handle non-Manhattan interconnect structures, we propose to use triangular discretization, as illustrated in Figure 2.

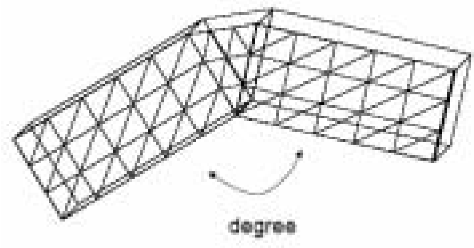

Figure 2: Triangular discretization.

To apply the triangular discretization, we shall present a new discretization method. There are 7 unknowns in a panel as follow: E_x, E_y, E_z, $\frac{\partial E_x}{\partial n}$, $\frac{\partial E_y}{\partial n}$, $\frac{\partial E_z}{\partial n}$, and ρ. Here, x, y, z are the axes of the space, n is the panel's normal vector, and ρ is the charge density. The scalar potential ψ is associated with the panel vertices.

If we use centroid collocation to discretize Equation (3), we have

$$P_1 \frac{\partial \vec{E}}{\partial n} - D_1 \vec{E} = 0, \qquad (8)$$

where

$$P_1(i,j) = \int_{panel_j} G_1(x_i, y) dy$$

and

$$D_1(i,j) = \int_{panel_j} \frac{\partial G_1}{\partial n}(x_i, y) dy,$$

where x_i is the circumcenter of the i^{th} panel.

Discretizing Equation (5), we can get a similar equation as above, with the only difference being with the gradient term $\nabla \psi$. For any panel, two independent tangential vectors can be found. As shown in Figure 3, two tangential directions t_a and t_b are formed by connecting a node and the midpoints of the sides. The representation of the tangential $\nabla \psi$ can be obtained using finite differences. Therefore, Equation (5) in the t_a direction can be transferred into

$$T_{t_a} P_0 \frac{\partial \vec{E}}{\partial n} - T_{t_a} D_0 \vec{E} + \nabla_{t_a} \psi = 0, \qquad (9)$$

$$P_0(i,j) = \int_{panel_j} G_0(x_i, y) dy,$$

and

$$D_0(i,j) = \int_{panel_j} \frac{\partial G_0}{\partial n}(x_i, y) dy,$$

where Tt_a is the transfer matrix related to the local coordinate system (t_a or t_b) to the global coordinate system (x, y, and z).

The gradient of ψ along t_a in Figure 3 can be computed by

$$\nabla_{t_a} \psi = \frac{\frac{\psi_\alpha + \psi_\gamma}{2} - \psi_\beta}{|\beta M_{\alpha\gamma}|} \qquad (10)$$

where ψ_α, ψ_β, and ψ_γ are the voltages of nodes α, β, and γ, respectively. $M_{\alpha\gamma}$ is the midpoint of nodes α and γ. $|\beta M_{\alpha\gamma}|$ is the length of line $\beta M_{\alpha\gamma}$. So we can find an A_{ta} matrix, which $A_{ta}\psi$ is equal to $\nabla_{ta}\psi$.

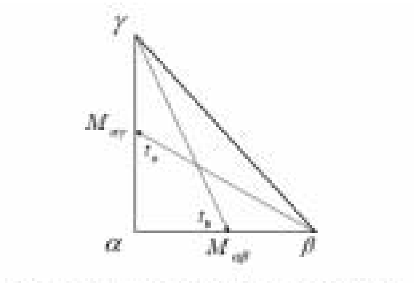

Figure 3: Computation of the gradient of potential.

In order to generate a set of equations for the vertex potentials, we consider applying the current conservation equation (6) to Figure 4. Node Q in the figure is the vertex at the intersection of the panels. First we find the circumcenter of every triangle, such as C_{P1}, C_{P2}, C_{P3}, C_{P4}, C_{P5}, and C_{P6}. Second, we connect these nodes to build another panel (see Figure 4), the region surrounded by dash lines. Applying the surface integral equation (6) to this region generates the following equation:

$$\int_P E_t(x) \cdot (n(x)) \times l(x)) dx - \int_S \frac{\partial E_n(y)}{\partial n(y)} dy = 0, \qquad (11)$$

where P is the perimeter of the region S enclosed by the dashed lines illustrated in Figure 4. For an arbitrary point x on P, $n(x)$ is the unit normal vector, and $l(x)$ is the unit vector along P.

Applying the aforementioned three boundary conditions, we can get the discretized form as follows:

$$N_{NC} \cdot \vec{E}_1 = \frac{i\omega\rho_1}{\sigma} \text{ (for non-contact panel [EMQS])}, \qquad (12)$$

$$N_C \cdot \frac{\partial \vec{E}_1}{\partial n} = 0 \text{ (for contact panel)}, \qquad (13)$$

and

$$F\psi = \psi_c \text{ (exciting voltage source)}, \qquad (14)$$

where N_{NC} and N_C are matrices formed by unit normal vectors at the non-contact and contact panels, and F is a matrix containing the potential information of the vertices.

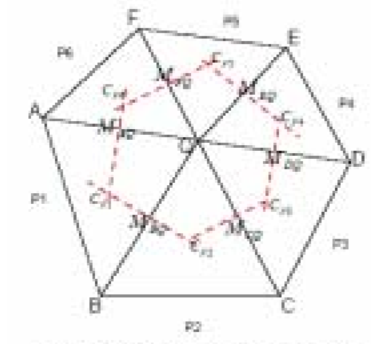

Figure 4: Panels of current conservation.

We can extend Equation (8) into three formulae for x, y, and z directions. Nevertheless, Equation (9) can only be extended into two formulae because there are only two independent tangential vectors on the panels, t_a and t_b. According to the above formulae, the system matrix can be derived as shown in Figure 5.

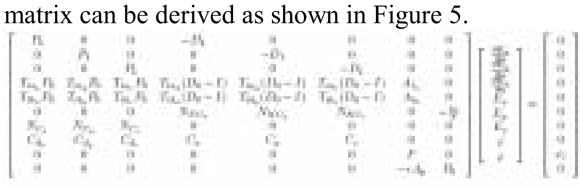
Figure 5: The system matrix.

After solving the system matrix by the iterative method, the coefficients of all parameters in each panel can be found. Then we can compute the incident current accordingly by the following equations:

$$J = \sigma E,$$

and

$$I = \int J ds = \sum_{panel_j \in C_+} -\sigma(n_+ \cdot E_j) s_j, \qquad (15)$$

where I is the incident current illustrated in Figure 6, J is the current density, s_j is the area of $panel_j$, and

$panel_j$ belongs to one of the contact surfaces.

In the boundary conditions, we make the voltage drop between two terminals be 1*v*. Therefore, we can compute the impedance Z by

$$Z = \frac{1}{I}, \quad (16)$$

and the inductance *Leff* by

$$L_{eff} = \frac{image(Z)}{\omega}.$$

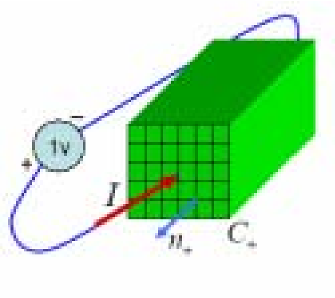

Figure 6: Current computation.

五、成果 (Publications)

1. C.-Y. Lai, S.-K. Jeng, and Y.-W. Chang, "Surface Integral Inductance Extraction for General Interconnect Structure," The 15th VLSI Design/CAD Symposium, Pingdong, Taiwan, Aug. 2004.
2. C.-Y. Lai, S.-K. Jeng, and Y.-W. Chang, "Parasitic Extraction for General Transmission Lines Based on Surface Integral and Triangular Discretization," submitted to ACM/IEEE Design Automation Conference, CA, June 2005.

六、參考文獻

[1] K. Banerjee and A. Mehrotra, "Analysis of On-Chip Inductance Effects using a Novel Performance Optimization Methodology for Distributed RLC," *Proc. DAC*, pp. 798–803, June 2001.

[2] A. Deutsch, A. Kopcsay, and G. V. Surovic, "Challenges Raised by Long On-Chip Wiring for CMOS Microprocessors," *Proc.IEEE Topical Meeting on Electrical Performance of Electronic Packing*, pp. 21-23, Oct 1995.

[3] D. S. Gao and D. Zhou, "Propagation Delay in RLC Interconnection Networks," *Int. Symposium on Circuit and Systems*, pp. 2125–2128, May 1993.

[4] Albert Guissard,"On the surface Field Integral Equations," *IEEE Trans. Education*, vol. 46, no. 4, Nov. 2003.

[5] L. He and K. M. Lepak, "Simultaneous Shield Insertion and Net Ordeing for Capacitive and Inductive Coupling Minimization," *Proc. ISPD*, pp. 55-60, 2000.

[6] Hongyu Chen, Bo Yao, Feng Zhou and Chung-Kuan Cheng, "The Y-architecture: yet another on-chip interconnect solution," *Proc. ASP-DAC,* pp. 840-846 Jan. 2003.

[7] J. Huang, B. song, J. K. White, and Z. Z. Hu, "Improving the Robustness of a Surface Integral Formulation for Wideband Impedance Extraction of 3D Structures." *Proc. ICCAD,* Nov. 2001.

[8] Y. I. Ismail and E. G. Friedman, "Effects of Inductance on propagation Delay and Repeater Insertion in VLSI Circuits," *IEEE Trans. VLSI System*, Vol. 9, Issue: 2, April 2000.

[9] D. B. Jarvis, "The Effects of Interconnections on High-Speed Logic Circuits," *IEEE Trans. Electronic Computers*, Vol. EC-10, No. 4, pp. 476-487, Oct. 1963.

[10] Junfeng Wang, "A new surface integral formulation of EMQS impedance extraction for 3-D structures," *Ph.D. thesis MIT EECS Department*, 1999.

[11] A. B. Kahng and S. Muddu, "Optimal Equivalent Circuits for Interconnect Delay Calculations Using Moments," *Proc. European Design Automation Conf.*, pp. 164–169, Sep. 1994.

[12] A. B. Kahng and S. Muddu, "Two-pole Analysis of Interconnection Trees," *Proc. MCMC Conf.*, pp. 105–110, Feb. 1995.

[13] A. B. Kahng and S. Muddu, "An Analytical Delay Model for RLC Interconnects," *IEEE Trans. CAD*, vol. 16, no. 12, pp. 1507–1514, Dec. 1997.

[14] M. Kamon, M. J. Ttsuk and J. K. White,"FASTHENRY: a multipole-accelerated 3-D inductance extracion program, " *IEEE Trans. Microwave Theory and Techniques,* Vol. 42 , Issue:9, pp. 1750-1758, Sept. 1994

[15] I. S. Kourtev and E. G. Friedman, *Timing Optimization Trough Clock Skew Scheduling*, Kluwer Academic Publishers, Massachusetts, 2000.

[16] R. G. Meyers and Ye Qiubo, "Incorporation of Zeland's IE3D in the microwave and RF classroom," *Antennas and Propagation Society International Symposium*, Volume: 1 , pp.688-691, June 2002

[17] Ankireddy Nalamalpu and Wayne Burleson, "Repeater Insertion in deep sub-micron CMOS: Ramp-based Analytical Model and Placement Sensitivity Analysis," *Proc. International Symposium on Circuits and Systems*, vol.3, pp. 766 -769, June. 2000.

[18] H. Nakashima, N. Takagi and K. Masu, "Derivation of interconnect length distribution in X architecture LSIs," *Proc. Interconnect Technology Conf.*, pp. 66-62, June 2003.

[19] "Semiconductor Industry Association," *International Technology Roadmap for semicondutors*, 1999.

[20] Semiconductor Industry Association, *International Technology Roadmap for Semiconductors 1999 Edition*, 1999.

[21] L. M. Silveira, M Kamon and J. K. White, "Efficient reduced-order modeling of frequency-dependent coupling inductances associated with 3-D interconnect structures," *Proc. European Design and Test Conf.*, March 1995

[22] M. Sriram and S. M. Kang, "Performance Driven MCM Routing Using a Second Order RLC Tree Delay Model," *Proc. IEEE Intl. Conf. on Wafer Scale Integration*, pp. 262-267, Jan. 1993.

[23] T. Sakurai and A. R. Newton, "Alpha-Power Law MOSFET Model and its Applications to CMOS Inverter Delay and Other Formulas," *IEEE Journal of Solid-State Circuits*, Vol. 25, No. 2, pp. 584-594, Apr. 1990.

[24] K. T. Tang and E. G. Friedman, "Delay and Power Expressions Characterizing a CMOS Inverter Driving an RLC Load," *Proc. the IEEE International Symposium on Circuits and Systems*, pp. III.283-III.286, May 2000.

[25] J. Torres, "Advanced Copper Interconnections for Silicon CMOS Technologies,"*Applied Surface Science*, Vol. 91, No. 1, pp. 112-123, Oct 1995.

[26] J. Wang and J. K. White, "A wide frequency range surface integral formulation for 3d RLC extraction," *Proc. ICCAD*, 1999.

[27] Jian-Xiong Zheng,"A general purpose 3D electromagnetic simulation and optimization package-IE3D," *Microwave Symposium Digest.*, IEEE MTT-S International , pp. 373-376, May 1994 .